# Geophysical experiments in periglacial environments: Devon Island, Nunavut

Carlos E. Nieto and Robert R. Stewart


## ABSTRACT

In the summer of 2003, various 2D and 3D ground-penetrating radar surveys were acquired at two different locations around the NASA Haughton–Mars Project base camp on Devon Island, Nunavut. The objective of the project was to obtain high–resolution images to understand shallow subsurface structure periglacial environments. We used a Sensors and Software Systems NOGGIN 250 MHz GPR equipment to record the data. It has a constant antenna separation of 0.28 m and allows a real–time display of the data that has been acquired.

A calibration experiment using rebar as a point diffractor was used to define a velocity model of the thawed layer of the area. We found an average velocity of 0.065 m/ns for this layer, which correlates with standard velocities reported for this type of material. At the same site, a 3D GPR over a 10 m$^2$ area shows the lateral distribution of the thawed–frozen ground interface. The thickness of this layer varies from 0.60 m to 0.78 m. Diffraction patterns at different locations are interpreted to be caused by the presence of ice lenses or cobbles at the permafrost top. An absence of data between adjacent lines in both direction of the 3D was solved by interpolation. A quasi–3D GPR was acquired at a site characterized by water saturation, which has the effect of supplying heat to the ground and is observed in this volume by a relatively deeper thawed–frozen ground interface. The depth values range from 0.7 m to 0.9 m.


## INTRODUCTION

The Haughton meteorite impact structure on Devon Island, Nunavut in the high Canadian Arctic is one of the most Mars-like places on Earth. The Haughton structure, at 75°22’N latitude and 89°41’W longitude, is a 23 Ma–old impact crater about 20 km in diameter (Cockell et al, 2001, and 2002). Host rocks of the structure are of Ordovician and Silurian age, mostly of the Allen Bay formation (Lee, 2002a). The impact has left a very impressive scar on the landscape as seen from an airborne radar image.

The northwest region of the outer middle rim hosts the base camp for the Haughton Mars Project (Figure 1; Lee, 2002b and 2002c; Long, 1999; Nieto et al., 2003). Geophysical surveying can be difficult, even in the summer on Devon Island, due to the high winds of the polar area (up to 70 km/hr during this field survey), low summer temperatures (-5°C to +5°C), sleet, rain, snow, even though this is characterized as a desert (Osinski et al., 2001a), and significant ultraviolet radiation (Osinski et al., 2001b).


FIG. 1. Map of North America showing the location of Devon Island, Nunavut (image from the NASA Haughton-Mars Project / www.marsonearth.org).

## GROUND–PENETRATING RADAR SURVEYS

Two different locations were chosen to survey with a NOGGIN 250 MHz ground-penetrating radar unit. The first survey site was a flat area located between the Greenhouse and the work tent: *"base camp"*, Figure 2. The next survey site was located to a side of a moderate steep hill close to the base camp: *"landing strip"*, Figure 3.

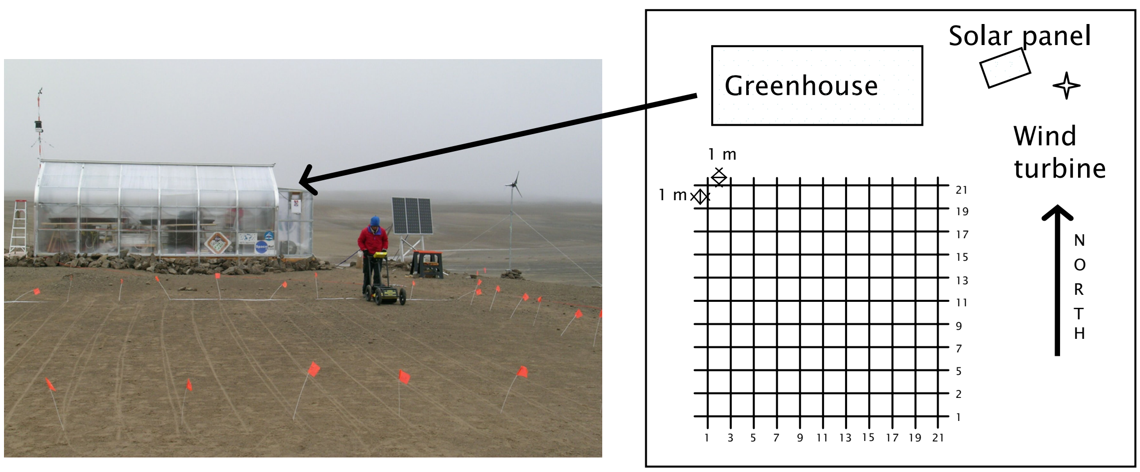


FIG. 2. Photograph of the base camp survey site and acquisition of the GPR lines using the NOGGIN 250 MHz cart. The diagram on the right shows a plan view of the survey site and 3D survey geometry.

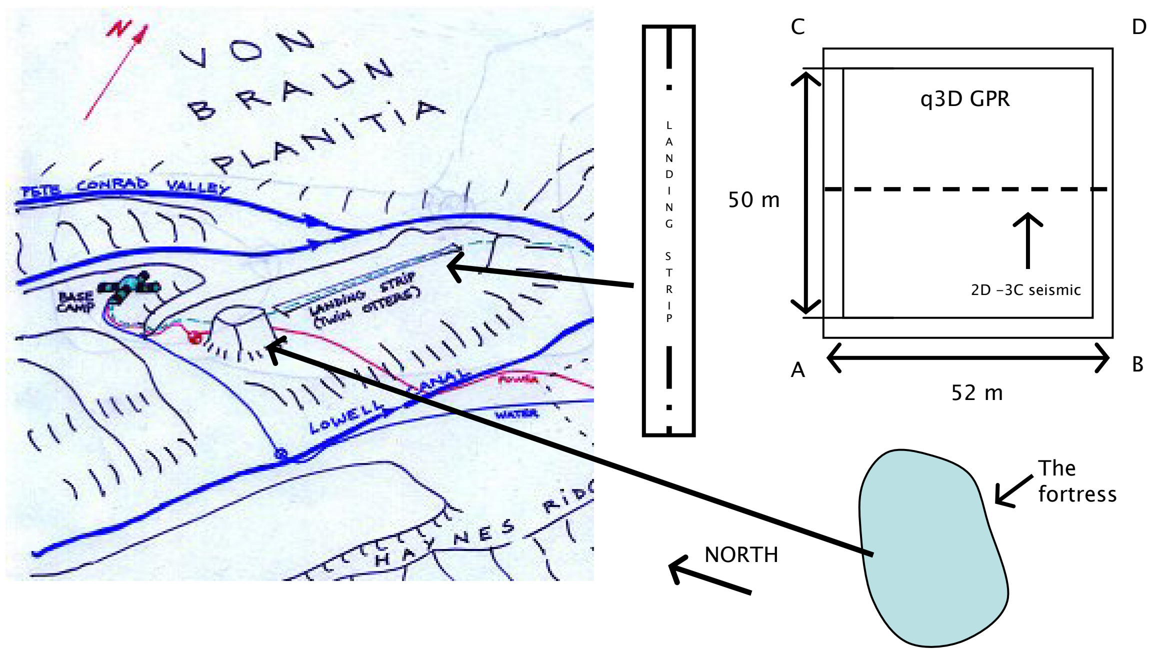


FIG. 3. View of the survey site by the landing strip. The left diagram is a perspective view of the base camp surroundings, including the landing strip (image from the NASA Haughton-Mars Project / www.marsonearth.org). The diagram on the right side shows the landing strip and the surveyed area.

## Base camp survey site – reconnaissance GPR line

At the base camp site we first recorded an exploration GPR line. The objective was to obtain a quick image of the structure of the thaw layer (Figure 4). This line allowed us to confirm the presence of a strong reflection between the thaw layer and the frozen ground.

A characteristic of this line is the presence of discontinuities in the interface thaw–frozen ground. This could be caused by the formation of ice lenses at the top of the permafrost. Water that percolates through the thawed layer reaches the frozen ground and could form ice lenses (French, 1996). It may also be due to the presence of boulders at the permafrost top.

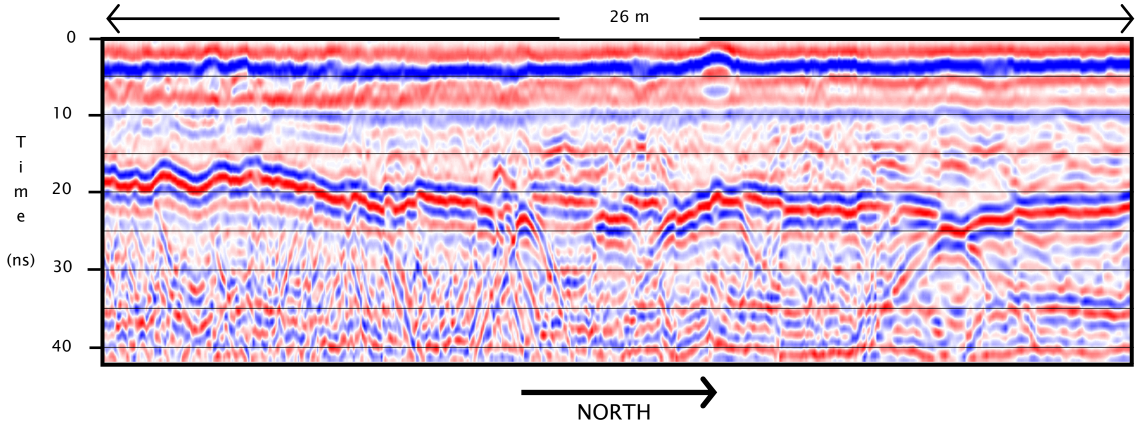


FIG. 4. GPR line from the base camp survey site. The line runs from the orange tent (left end) to the Greenhouse (right end). From left to right we observe the thickening of the thaw layer. At the centre of the line a series of diffractions are interpreted as ice lenses forming in the top of the permafrost.

Moorman et al. (2000) shows that the reflection coefficient for a planar surface is given by:

$$R = \frac{\sqrt{k_1} - \sqrt{k_2}}{\sqrt{k_1} + \sqrt{k_2}} \tag{1}$$

The constants $k_i$ represents the dielectric constant of the material and are measured in electrostatic units (esu). For unfrozen sediment the average k is 25 esu, while for frozen sediment is 6 esu. The reflection coefficient for this case scenario is 0.34. This value is very high compared to the frozen sediment (k=6 esu) to rock (k=8 esu) case which has a reflection coefficient of -0.07.

**Base camp survey site – calibration test, "rebar experiment"**

At the base camp site a calibration test was acquired (Figure 5). The experiment consisted in recording a 6 m line across pounded rebar pounded into undisturbed sediment at various depths in order to determine the velocity profile of the thawed layer.

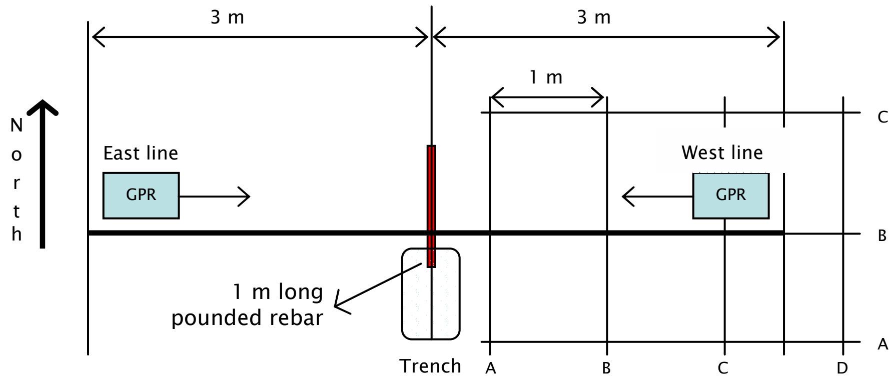


FIG. 5. Diagram showing the location of the calibration experiment. The line was recorded at the southeast corner of the base camp survey site.

The experiment started by digging a trench until frozen ground was reached (assumed to be the top of the permafrost). The depth at which this occurs is about 60 cm. A one–metre rebar was pounded at various depths into one of the sides of the trench (Figure 6).

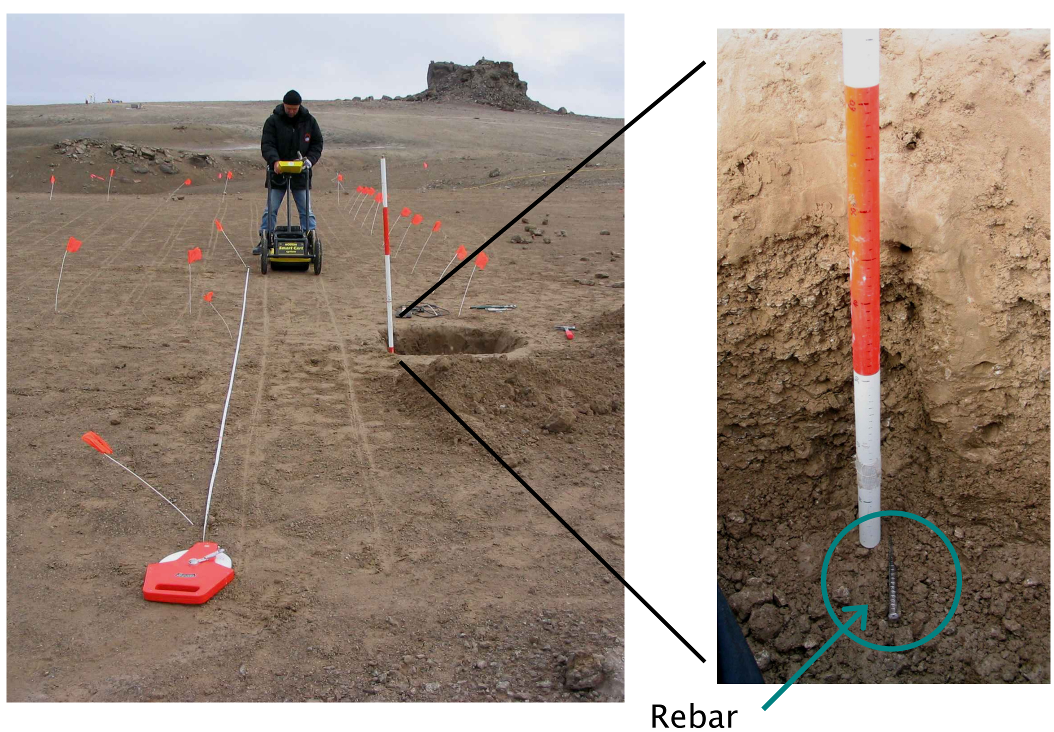


FIG. 6. Calibration test for ground–penetrating radar. A 6–m–long line was recorded for various depths of the pounded rebar. The person in the left picture is controlling the GPR cart. The right picture shows one end of the pounded rebar in the trench. The length of the rebar was approximately one metre.

The depths at which rebar was pounded were 0, 10, 20, 30, 40, 50, and 62 cm. For each case two lines in opposite directions were recorded and an additional line with no rebar was recorded as well (Figure 7). A standard processing flow was used to enhance the diffraction patterns: trace DC removal, automatic gain control (10 ns operator), and high–cut frequency filter (560 MHz).

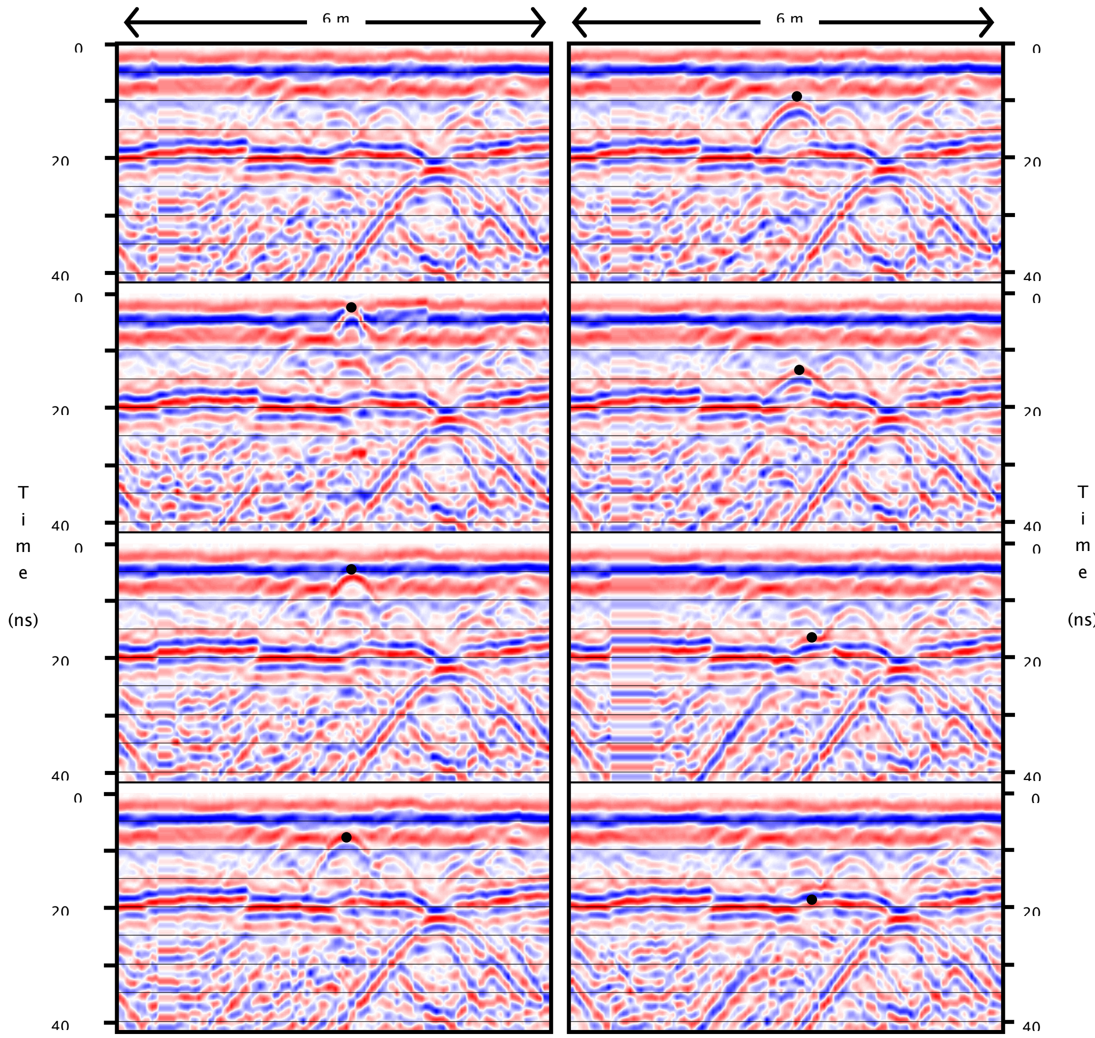


FIG. 7. Results from the calibration experiment at the base camp survey site. From top to bottom, the left column sections correspond to: no rebar, rebar @ surface, rebar @ 0.1 m, and 0.2 m; and the right column section correspond to: rebar @ 0.3 m, 0.4 m, 0.5 m, and 0.62 m. These lines are oriented from east to west. The rebar is identified by a diffraction marked with a black dot.

The events interpreted in the GPR sections are: (1) a horizontal interface which corresponds to the air wave interfering with the ground wave, (2) followed by a strong close to horizontal event (at 20 ns) that corresponds to the reflection from the frozen–thawed interface.

Using the time–depth values from each experiment, Table 1, we estimated interval velocities as well average radar velocities for the thawed layer (Figure 8). Interval velocities were obtained by calculating the slope between two adjacent time–depth values, Table 1. From these values we calculate an RMS velocity curve that shows the expected decreasing trend below 0.2 m deep (Figure 9). A third velocity model was obtained by fitting hyperbolas to the diffractions at various depths (Figure 9).

Table 1. Radar velocities obtained from rebar calibration test. The times are referred to the zero time of 10.32 ns specified by the NOGGIN 250 MHz equipment.

| Rebar depth (m) | Rebar time (ns) | Interval velocity (m/ns) | RMS velocity (m/ns) | Diffraction velocity (m/ns) |
|---|---|---|---|---|
| 0.00 | 2.98 | 0.0577 | 0.0577 | 0.0430 |
| 0.10 | 5.95 | 0.0672 | 0.0626 | 0.0565 |
| 0.20 | 7.54 | 0.1260 | 0.0802 | 0.0575 |
| 0.30 | 10.32 | 0.0720 | 0.0781 | 0.0630 |
| 0.40 | 13.50 | 0.0630 | 0.0748 | 0.0640 |
| 0.50 | 16.67 | 0.0630 | 0.0727 | 0.0705 |
| 0.62 | 20.24 | 0.0672 | 0.0718 | 0.0740 |

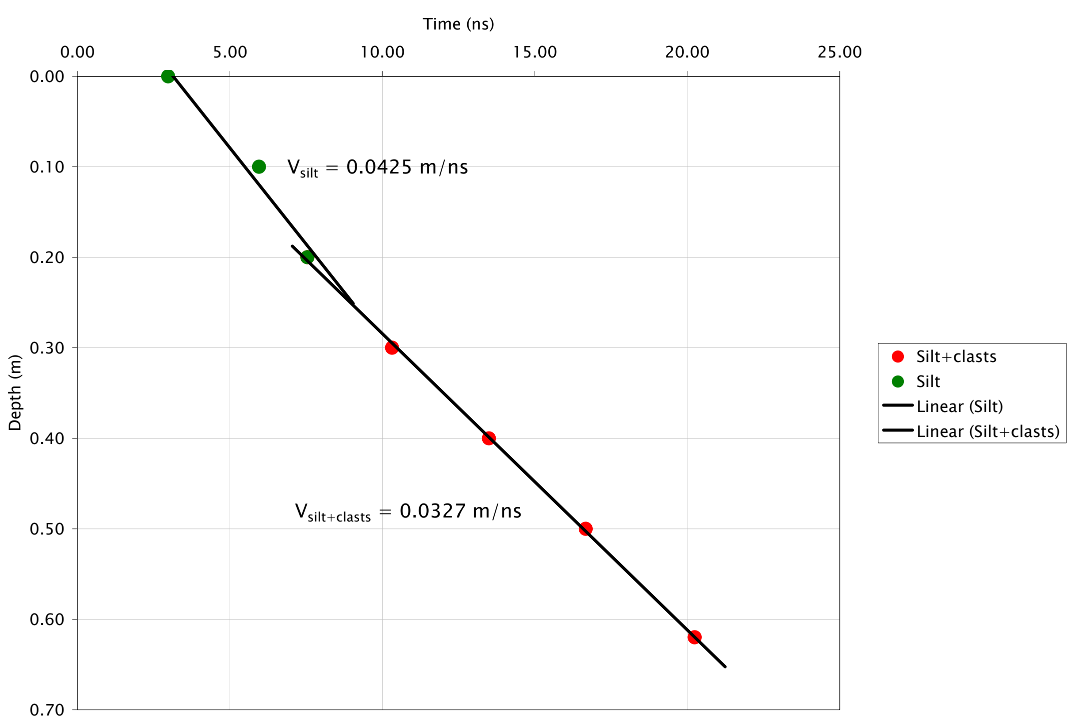


FIG. 8. Time–depth values from the rebar calibration test. A change in the velocity structure is observed at approximately 0.20 m. This correlates to the change in lithology observed in the pit.

A slight change in the slope is observed in both the velocity model and the lithological profile (Figures 8, 9, and 10) at 0.20 m approximately. It is interpreted to be caused by a change in water content at the near surface. Radar velocity of water is 0.033 m/ns approximately (Moorman et al., 2000), which makes it slower at the surface. Velocity values obtained for the thawed layer compare to standard values reported in Davis and Annan (1989).

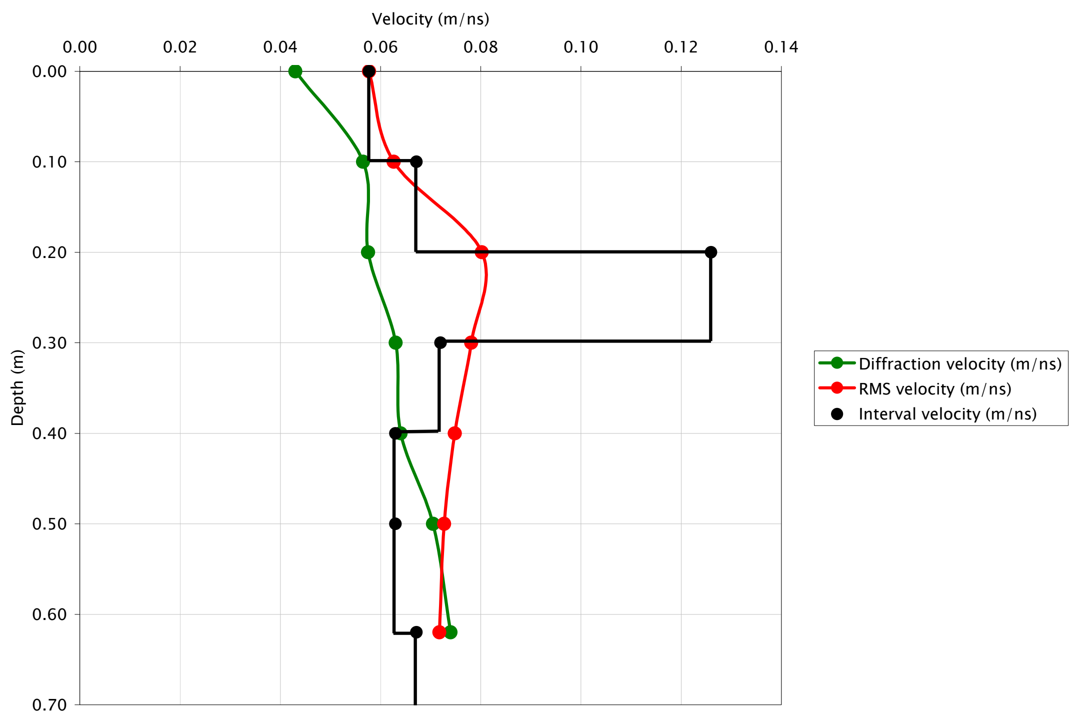


FIG. 9. Velocity (m/ns) versus depth (m) display. The blue curve is the velocity obtained from matching hyperbolas to diffractions. The black line represents the velocity model from interval velocities. The difference in velocity in the shallow part of the graph is caused by water content in the near surface.

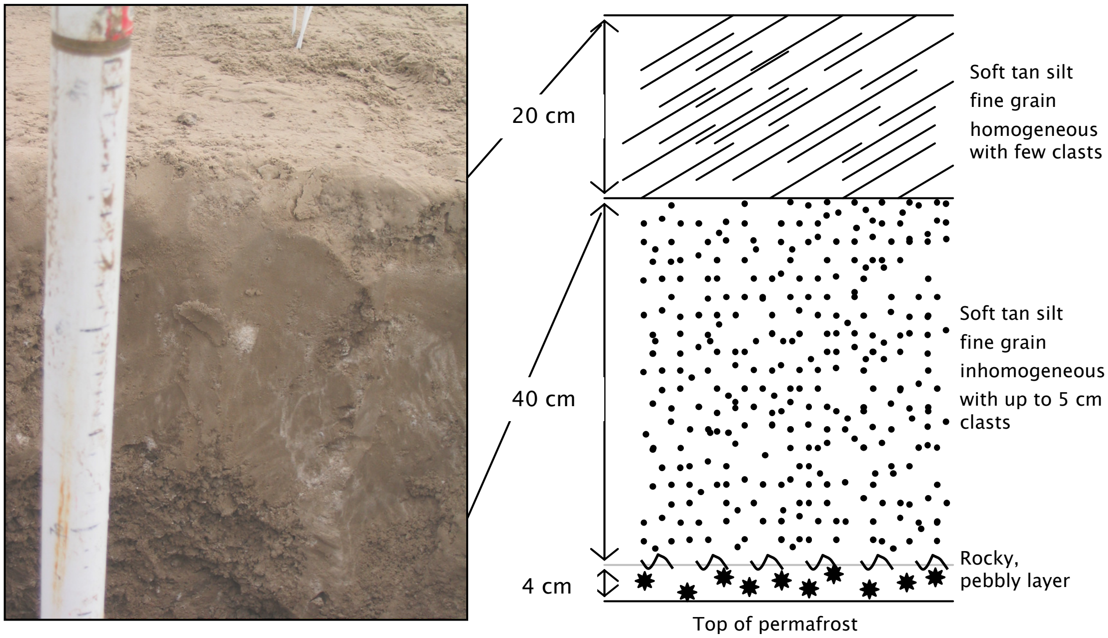


FIG. 10. Thawed ground profile from the experimental pit. The lithology consists of three units: fine silt, silt with clasts, and rocky layer. At 20 cm deep a noticeable change in lithology is observed.

## Base camp survey site – 3D GPR

A total area of 10 $m^2$ was surveyed using the NOGGIN 250 MHZ cart (Figure 2). The grid consisted of 21 north–south lines and 21 east–west lines. It was acquired using a forward–reverse survey type. The spatial sample rate used was 0.05 m, the time–sample rate was 0.397 ns; and the length of the lines was 10 m. We started recording the north–south lines and then continued with the east–west (Figure 11). A reduction of the radar velocity in the top few centimetres of the surface is expected due to rain.

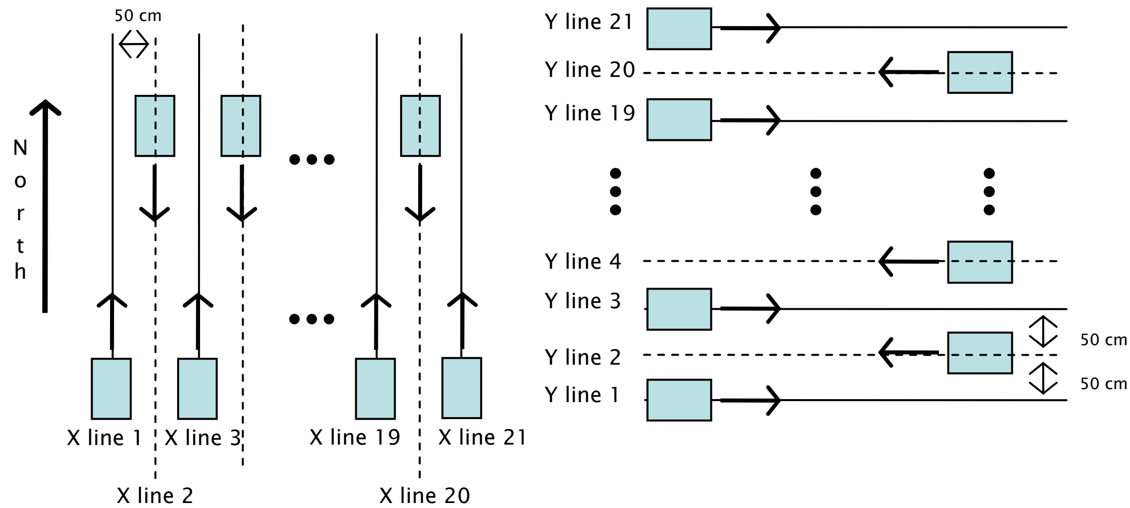


FIG. 11. 3D GPR survey at the base camp. The grid consisted of 21 x 21 lines spaced 0.5 m. The north–south direction is defined as *inline* and the east–west the *crossline*.

The geometry preparation for the 3D consisted of

(1) Reversing the trace number for the even lines for both X and Y lines

(2) For X lines use:

INLINE header value = channel number

CROSSLINE header value = 1 + 10 x (shot line – 1)

And for Y lines:

INLINE header value = 1 + 10 x (shot line – 1)

CROSSLINE header value = channel number

(3) Combine X and Y lines, averaging coincident traces.

The processing flow used for the rebar experiment was applied for this 3D. No migration process has been applied. The result is a volume with a 10 $m^2$ area (Figure 12).

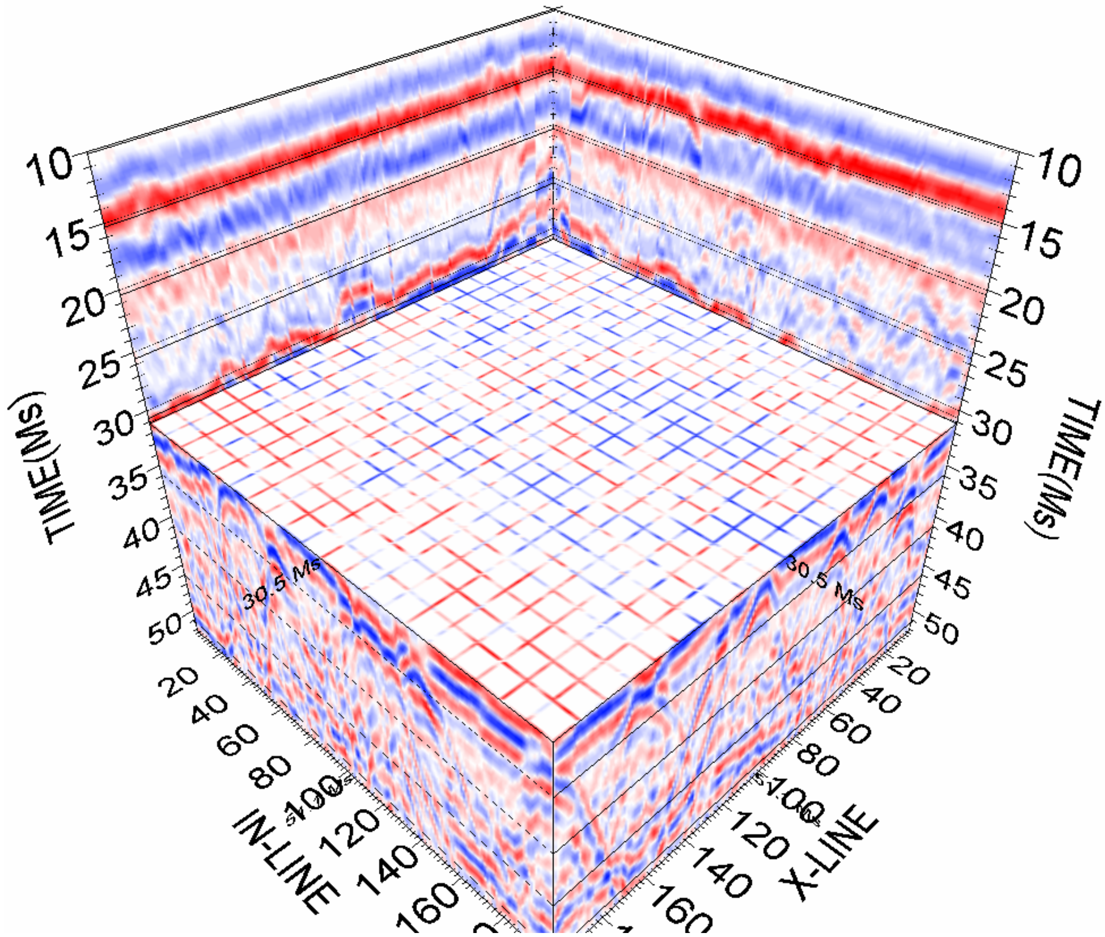


FIG. 12. GPR volume from the base camp survey site. The origin of the coordinates is located behind the displayed cube. The timescale is in nanoseconds instead of milliseconds, and from 0 to 40 instead of 10 to 50. North lies towards the greater inline values. The time slice is at 30 ns.

The product from this survey is a GPR volume that shows both the vertical and the horizontal extent of the features observed in the reconnaissance line (Figure 4). Depending on the objective of the 3D, different visualization techniques can be applied for further analysis. At the moment we are interested on the structure of the thawed layer and the interface between unfrozen–frozen ground.

In this volume, we can observe the presence of the ground wave (marking the surface), and a later event corresponding to the interface thawed–frozen ground (Figure 12). An additional event can be recognized at 47 ns approximately, which may be interpreted as a relic active layer–permafrost interface. A diffraction pattern observed in both directions of the volume is attributed to ice accumulations at the top of the frozen layer.

The model interpreted from this volume consists of:

(1) Variable thickness thawed layer. Thickness ranges around 65 cm.

(2) Frozen ground with ice lenses at the top formed by water percolating from the surface.

(3) A possible relic active layer–permafrost interface at 47 ns approximately.

An issue with this data set is the absence of traces between adjacent lines (Figure 12). Averaging from 2 to 10 traces the volume was used to analyze the image from high resolution to low resolution (Figure 13).

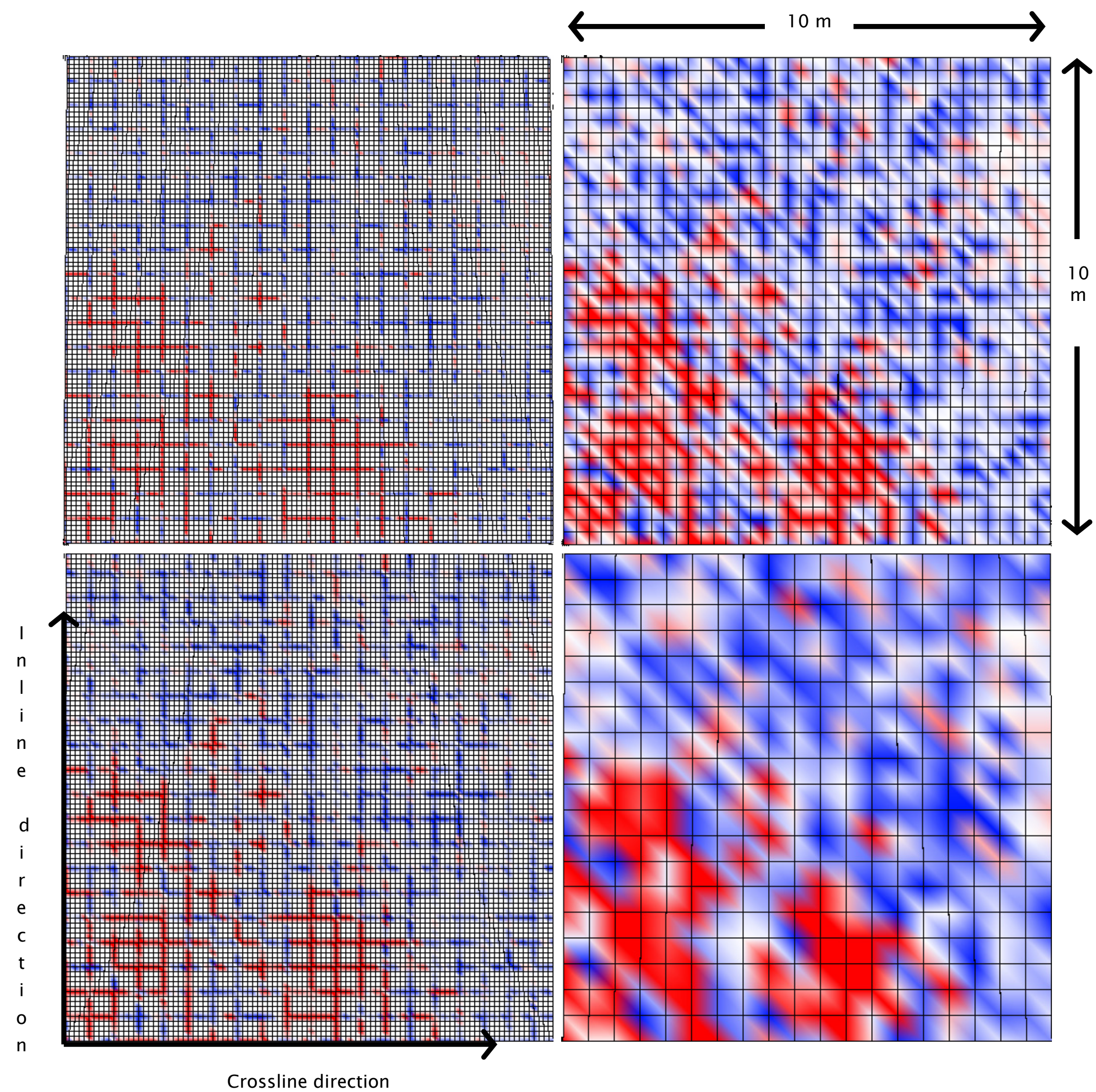


FIG. 13. Time slices at 28 ns from the base camp 3D GPR survey. From top to bottom, the first column has no average, and below a two–trace average. The right column has a 5–traces average, and below a 10–trace average.

Further processing techniques are required to extend the analysis of the data, including: (1) migration to collapse and enhance the image; (2) interpolation to obtain a continuous plan view, (3) further filtering techniques.

### Landing strip survey site – quasi–3D GPR

A quasi–3D GPR survey consisting of a set of only north–south lines was acquired at this site. We used the forward–reverse recording mode for this survey as well. The grid for this survey consisted of eleven lines in the north–south direction, spaced at 5 m (Figure 14).

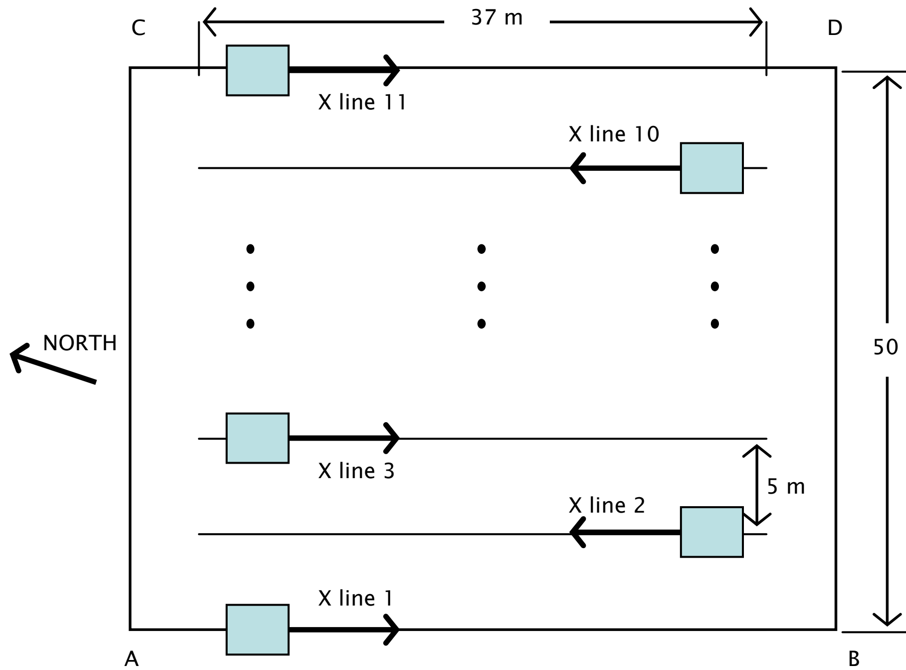


FIG. 14. Diagram showing the grid for the quasi–3D GPR at the landing strip survey site. A total of eleven lines were recorded in the north–south direction. The perimeter ABDC was also surveyed with GPR. The north–south direction is considered to be the *inline* direction.

The geometry and processing for this data set is equal to the flow used for the 3D GPR at the base camp site, with the difference that only one direction was recorded. A volume was also obtained for this survey (Figure 15). Continuity in the crossline direction (east–west) is worse in this case due to the line spacing (Figure 14). The thawed layer of the survey site was saturated with water varying from high saturation towards the landing strip. The water acts as a heat source, causing the thaw layer to thicken as water content increases. This effect is reflected across the volume from this site (Figure 15).

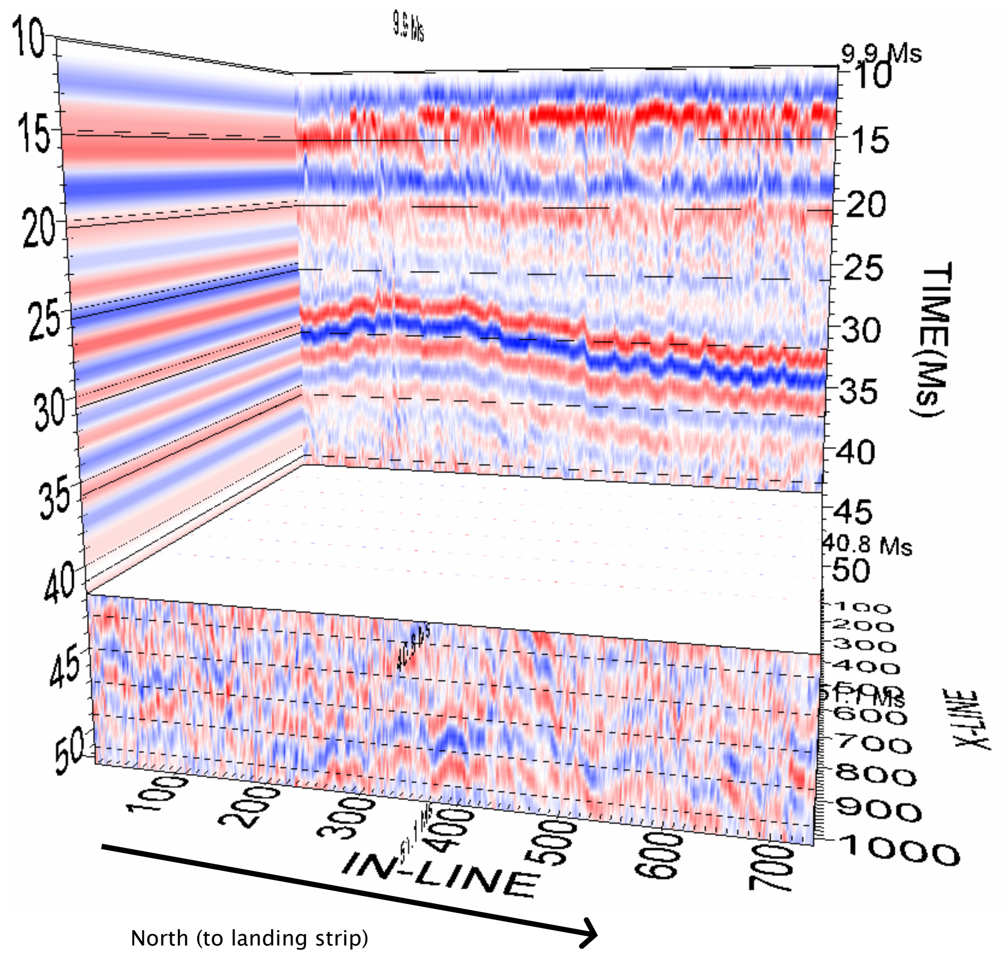


FIG. 15. GPR volume from the landing strip survey site. The origin of coordinates is located behind the displayed cube. The timescale is in nanoseconds instead of milliseconds, and from 0 to 40 instead of 10 to 50. North lies towards the greater inline values. Time slice is at 40 ns.

## CONCLUSIONS

Ground–penetrating radar 2D and 3D surveys were acquired at two different locations in the Haughton–Mars Project base camp in Devon Island, Nunavut. A first line shows a thawed layer marked by a strong reflection. The contrast between the dielectric properties of frozen to thawed ground is key to using GPR techniques for near–surface exploration in periglacial environments.

A calibration experiment that consisted of recording GPR lines with pounded rebar at various depths was acquired. This survey allowed the definition of a radar velocity model of the thawed ground. Values vary around 0.065 m/ns inside this layer, which correlates with standard velocities reported in the literature.

At the same site, a 3D GPR over a 10–m$^2$ area was acquired. The horizontal distribution of the thawed–frozen ground interface was obtained. The thickness of this layer varies from 0.60 m to 0.78 m. Diffraction patterns at different locations are interpreted to be caused by the presence of ice lenses at the permafrost top. An absence of data between adjacent lines in both direction of the 3D was solved by interpolating and averaging.

The second survey site was located to the side of the landing strip. The surface was characterized by being saturated with water. This had the effect of supplying heat to the ground. A set of eleven lines in the north–south direction was acquired at this location. The length of the lines was 37 m. A quasi–3D was conformed from this data set, and the thawed–frozen ground was observed at a depth range from 0.7 m to 0.9 m. Interpolation techniques are required to obtain a high–resolution image in this and the previous case.

## ACKNOWLEDGEMENTS

We express our appreciation to the NASA Haughton–Mars Project and especially its principal investigator, Dr. Pascal Lee of NASA Ames. Thank you to Sensors and Software Inc. for GPR support. Many thanks to Mssrs. Eric Gallant and Henry Bland of the CREWES Project at the University of Calgary who provided logistical help. We thank the University of Calgary (especially former Department Head, Dr. Don Lawton) for equipment support. Many thanks also to our Inuit helpers: Sam, Jon, and Pauline; and to Melanie and all the people involved in the Haughton–Mars Project. This work was partially supported by R. Stewart's NSERC Discovery Grant.

## REFERENCES

Cockell, C.S., Lee, P., Schuerger, A.C., Hidalgo, L., Jones, J.A., and Stokes, M.D., 2001, Microbiology and vegetation of micro–oases and polar desert, Haughton impact crater, Devon Island, Nunavut, Canada: Arctic, Antarctic, and Alpine Research, **33**, 306–318.

Cockell, C.S., Scherer, K., Horneck, P., Rettberg, P., Facius, R., Gugg-Helminger, A., Driscoll, C., and Lee, P., 2002, Exposure of Arctic field scientists to ultraviolet radiation evaluated using personal dosimeters: Photochemistry and Photobiology, **74**, 570–578.

Davis, J.L. and Annan, A.P., 1989, Ground–penetrating radar for high–resolution mapping of soil and rock stratigraphy: Geophysical Prospecting, **37**, 531–551.

French, H.M., 1996, The Periglacial Environment: Addison Wesley Longman Ltd.

Lee, P., 2002a, Mars on Earth: The NASA Haughton–Mars Project: Ad Astra, National Space Society, **14**, 12–17.

Lee, P., 2002b, From Earth to Mars, Part One: A crater, ice, and life: The Planetary Report, Vol. 1.

Lee, P., 2002c, From Earth to Mars, Part Two: Robots and humans working together: The Planetary Report, Vol. 1.

Long, M.E., 1999, Mars on Earth: National Geographic, **196**, 34-51.

Moorman, B.J. and Michel, F.A., 2000, Glacial hydrological system characterization using ground–penetrating radar: Hydrological Processes, **14**, 2645–2667.

Nieto, C. and Stewart, R.R., 2003, Ultra-high seismic and GPR imaging of permafrost: Devon Island, Nunavut: CSPG/CSEG National Convention, Calgary.

Osinski, G.R. and Spray, J.G., 2001a, Impact-generated carbonate melts: evidence from the Haughton structure, Canada: Earth and Planetary Science Letters, **194**, 17-29.

Osinski, G.R., Spray, J.G., and Lee, P., 2001b, Impact-induced hydrothermal activity within the Haughton impact structure, arctic Canada: Generation of a transient, warm, wet oasis: Meteoritics and Planetary Science, **36**, 731-745.